Annales Societatis Geologorum Poloniae (2012), vol. 82: 331–347.

MICROBIAL LAMINITES WITH COPROLITES FROM UPPER JURASSIC CARBONATE BUILDUPS (KRAKÓW–CZĘSTOCHOWA UPLAND, POLAND)

Alicja KOCHMAN & Jacek MATYSZKIEWICZ

Faculty of Geology, Geophysics and Environment Protection, AGH University of Science and Technology, Al. Mickiewicza 30; 30-059 Kraków, Poland; e-mails: kochman@geol.agh.edu.pl, jamat@geol.agh.edu.pl

Kochman, A. & Matyszkiewicz, J., 2012. Microbial laminites with coprolites from Upper Jurassic carbonate buildups (Kraków–Częstochowa Upland, Poland). *Annales Societatis Geologorum Poloniae*, 82: 331–347.

Abstract: The Upper Oxfordian microbial-sponge agglutinated to open-frame reef complex of the Zegarowe Crags in the Kraków–Częstochowa Upland originated upon an elevation of the Late Jurassic stable northern shelf of the Tethys. This elevation was formed, owing to a local decrease in subsidence rate during Jurassic time, induced by the presence of a Palaeozoic granitoid intrusion in the shelf substratum, and Late Jurassic, synsedimentary tectonics, which controlled the topography of the sea bottom. The Zegarowe Crags (Skały Zegarowe) complex at the top contains microbial laminites, composed of peloidal and agglutinated stromatolites, and intercalations of grainstones with indeterminable, favrenoid coprolites, occurring in large numbers. The development of stromatolites was associated with low nutrient availability. In contrast, the periodic activity of crabs, the main producers of the coprolites, forming the coprolitic grainstone intercalations, indicates periods, when nutrients were abundant in the sea water. The nutrinets most likely were associated with the occurrence of clouds of suspended matter, induced by gravity flows, generated by active, synsedimentary tectonics. The results of isotopic studies do not support the presence of warm, mineralizing solutions, connected with synsedimentary tectonics during development of the Zegarowe Crags complex in the Late Jurassic.

Key words: microbialites, coprolites, carbonate buildups, nutrients, synsedimentary tectonics, Oxfordian.

Manuscript received 25 October 2012, accepted 20 December 2012

INTRODUCTION

The Upper Oxfordian carbonate buildups, occurring commonly on the Kraków–Częstochowa Upland, are composed mainly of microbialites and subordinately of calcified, siliceous sponges. The carbonate buildups developed at moderate depth on the stable, northern shelf of the Tethys margin. A long period of erosion, to which these complexes have been subjected since the Late Jurassic period, resulted in the removal of the uppermost parts of them. Only exceptionally, there are deposits in the uppermost part of the carbonate buildups, which indicate a local change in sedimentary conditions (Matyszkiewicz, 1996; Matyszkiewicz & Krajewski, 1996).

The Upper Oxfordian Zegarowe Crags complex contains unusual, microbial laminites, with indeterminable, favrenoid coprolites, occurring in large numbers at the top (Matyszkiewicz et al., 2004, 2006a). These laminites are not known from other Upper Jurassic carbonate buildups on the Kraków–Częstochowa Upland and their occurrence appears to be linked to the emergence of specific conditions of sedimentation.

The present account outlines the development of microbial laminites, containing crab coprolites. The results of microfacies analysis, as well as geochemical and isotopic studies, provided the basis for a discussion of the possible, local occurrence of hydrothermal vents on the Late Jurassic shelf. These may have been close to active faults, related to Palaeozoic fault zones, which could have affected sediment deposition and the development of a distinctive, benthic fauna in the vicinity of seeps.

GEOLOGICAL SETTING

The Kraków–Częstochowa Upland is part of the Upper Cretaceous–Palaeogene Silesian-Kraków homocline, built up of Triassic, Jurassic and sporadically preserved patches of Cretaceous rocks, which are exposed at the surface (Fig. 1). These strata dip a few degrees to the NE and are underlain by folded, Palaeozoic rocks. The latter are cut by the Kraków–Lubliniec fault zone (Buła, 1994; Żaba, 1994, 1996, 1999; Buła *et al.*, 1997; Pulina *et al.*, 2005) of regional importance (Fig. 1). This zone marks the boundary between the terrane-

Fig. 1. Position of Upper Oxfordian complex of microbial-sponge buildups in Zegarowe Crags (asterisk) on geological structure of Kraków–Częstochowa Upland (based on Pulina *et al.*, 2005; modified and supplemented)

like Upper Silesian and Małopolska blocks. The Kraków–Lubliniec fault zone (KLFZ), particularly in the marginal part of the Małopolska Block, is accompanied by numerous, Palaeozoic granitoid and porphyry intrusions (Buła, 2002; Buła and Habryn, 2011). The KLFZ has been active since the Early Palaeozoic up to the present (Żaba, 1995; Moczydłowska, 1997), and the numerous faults, cutting the Mesozoic strata, frequently mimic trends of Palaeozoic deformation (Buła, 1994; Żaba, 1999; Pulina *et al.*, 2005).

The Zegarowe Crags form part of the Smoleń–Niegowonice Range, which extends roughly W–E across the Kraków-Częstochowa Upland (Poland), between the villages of Smoleń and Niegowonice. The Oxfordian complex of the Zegarowe Crags is situated on the eastern side of the Dolina Wodąca valley, about 5 km NW of Wolbrom (Figs 1, 2).

The Zegarowe Crags are situated within the Smoleń horst (Bukowy, 1968; Bukowy and Ślósarz, 1975), which is bounded by fault zones of roughly W–E orientation (Fig. 3) and with throws of up to about 250 m (Pulina *et al.*, 2005). The Upper Oxfordian strata, exposed in this area, belong to the so-called Smoleń massive limestones and subordinately to the Smoleń chalky limestones (Bednarek *et al.*, 1978; Pulina *et al.* 2005). The massive limestones, which predominate in this region, are about 100 m thick, but within tectonic grabens, the thickness of the Upper Jurassic strata increases to 200 m (cf. Kutek *et al.*, 1977; Bednarek *et al.*, 1985). The rocks, filling the tectonic grabens, are represented mainly by gravity-flow deposits (Bednarek, 1974; Bednarek *et al.*, 1978; Vierek *et al.*, 1994; Vierek, 1997; Matyszkiewicz *et al.*, 2006a). The gravity flows could have been triggered by both bottom relief and synsedimentary, tectonic movements during the Late Oxfordian (Bednarek *et al.*, 1985; Kutek and Zapaśnik, 1992; Vierek *et al.*, 1994; Matyszkiewicz *et al.*, 2006a). According to Pulina *et al.* (2005), the orientation of faults within the Upper Jurassic rocks in the Smoleń horst area is related to still active, deep-seated fault zones, reaching the Palaeozoic substratum.

The Smoleń–Niegowonice Range is typified by the presence of numerous caves; some of them are interpreted as being the result of hydrothermal karst processes (cf. Pulina

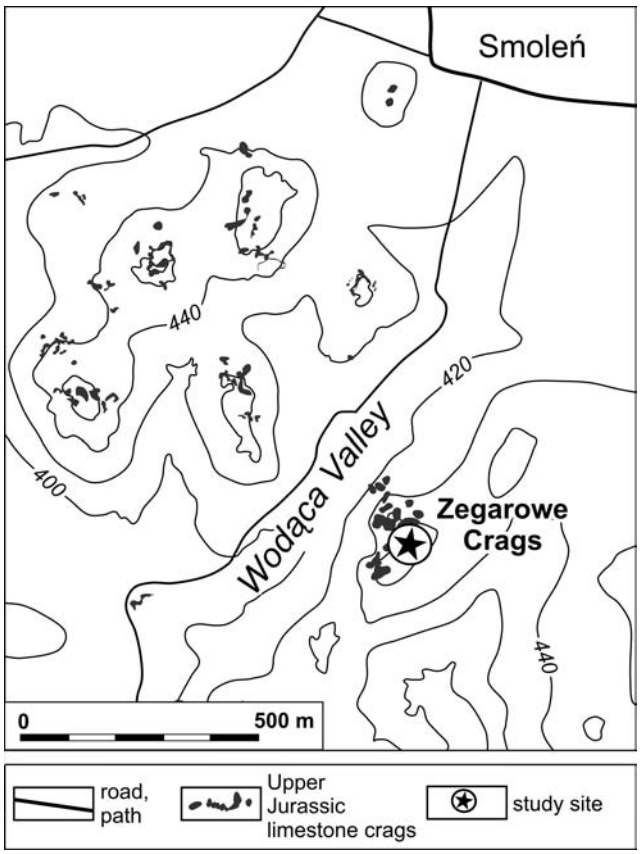

Fig. 2. Localization of Upper Oxfordian complex of microbial-sponge buildups in Zegarowe Crags

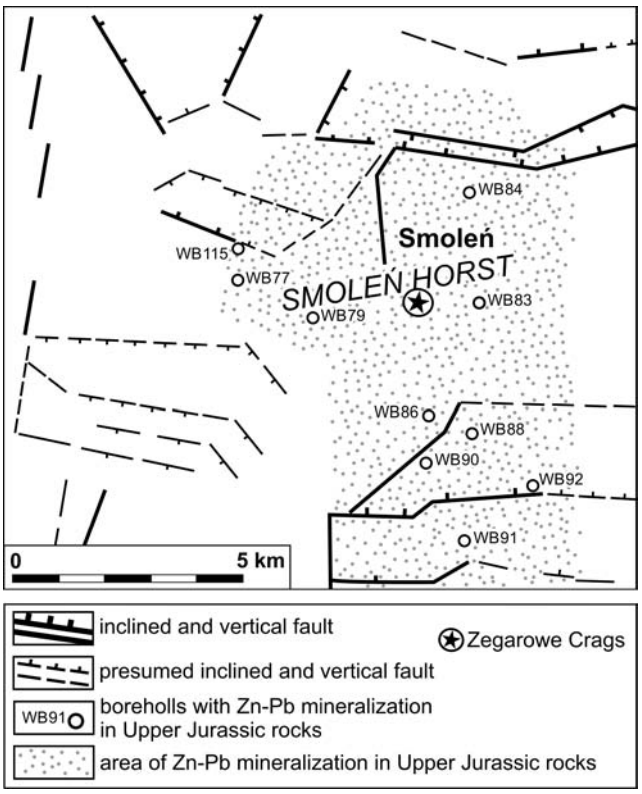

Fig. 3. Faults, cutting Upper Jurassic rocks, close to microbial-sponge buildups at Zegarowe Crags and area showing, Zn-Pb mineralization in Upper Jurassic rocks, detected in boreholes (after Bednarek *et al.*, 1985; simplified)

et al., 2005; see also Gradziński *et al.*, 2009). The position of these caves is related to the trace of KLFZ. The distinct traces of hydrothermal processes indicate the proximity of still active, deep-seated fault zones, associated with the KLFZ and suitable for circulation of warm, mineralizing fluids (Pulina *et al.*, 2005). Hydrothermal activity, related to the KLFZ, resulted in the formation of extensive, spring-fed freshwater limestones during the Late Triassic (Szulc *et al.*, 2006). Moreover, the Upper Jurassic rocks that surround the Zegarowe Crags on the KLFZ commonly contain dispersed ore minerals (Fig. 3), which are very much like those of the Zn-Pb ore deposits in the Triassic rocks (Bednarek *et al.*, 1985). Sphalerite, occurring in the Oxfordian rocks, shows homogenization temperatures of inclusions of 70–85 °C, whereas quartz veins indicate temperatures in the order of 80–90 °C (Bednarek *et al.*, 1985). Jacher-Śliwczyńska and Schneider (2004), on the basis of Pb-Pb isotopic studies of sphalerite and galena, maintain that the Zn-Pb deposits originated 150–200 million years ago (cf. Dżułyński and Sass-Gustkiewicz, 1982, 1985).

The Zegarowe Crags are dominated by limestones, representing a complex of microbial-sponge carbonate buildups. The Zegarowe Crags complex developed upon an elevation of the Late Jurassic, stable, northern shelf of the Tethys. Intensive growth of this complex was strongly controlled by structural properties of the bedrock. It formed, because of (1) a local decrease in the subsidence rate in Jurassic time, induced by the presence of a Palaeozoic granitoid intrusion in the shelf substratum (Matyszkiewicz *et al.*, 2006b), and (2) synsedimentary tectonics, active in the Late Jurassic, which contributed to relief differentiation of the sea bottom (Matyszkiewicz *et al.*, 2004, 2006a). Microbial-sponge carbonate buildups of the Zegarowe Crags complex, initially developing as sediment-starved mounds on fault-controlled, intraplatform highs, under a very restricted background sedimentation rate, were replaced by agglutinated microbial reefs (Matyszkiewicz *et al.*, 2004, 2006a). The successive stages of development of carbonate buildups in the Zegarowe Crags include: colonisation, aggradational growth, and progradation phases. In the colonisation phase, micritic peloidal thrombolites with siliceous sponges developed on top of loose peloidal-ooid sands. Peloidal and agglutinated thrombolites and stromatolites proliferated during the aggradational growth phase, whereas the progradation phase was characterized by shallowing and related development of microbial mats, composed of agglutinated stromatolites with favrenoid coprolites (Matyszkiewicz *et al.*, 2004, 2006a).

METHODS AND TERMINOLOGY

The main research method was microfacies analysis of 30 oriented thin and polished sections. Samples were collected from an approximately 1.5 m thick section of the uppermost part of the Zegarowe Crags (Figs 4, 5). In polished sections, under the binocular microscope, the position of the

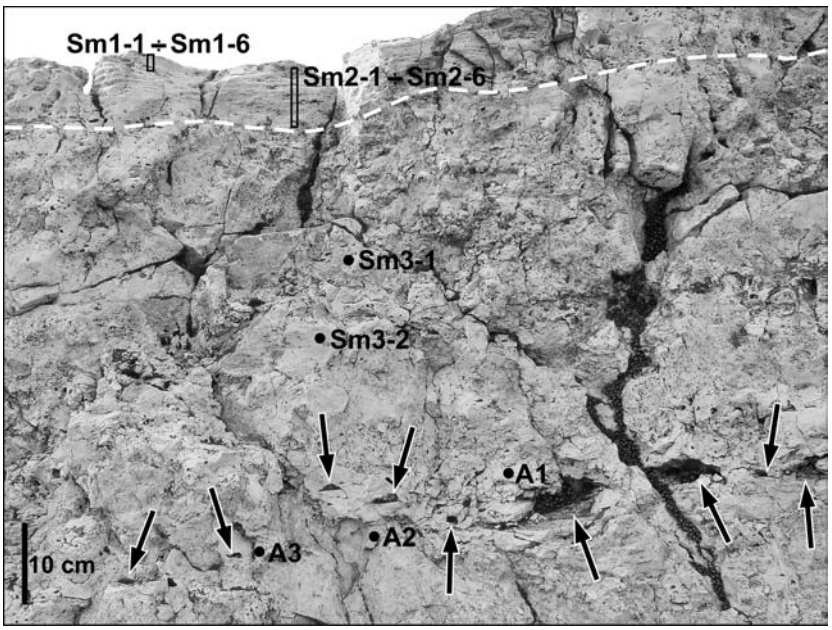

Fig. 4. Top part of Zegarowe Crags. Laminated limestone, composed of microbial mats, intercalated with coprolitic grainstone, visible at top. Dashed line marks base of limestone. Underlying rock is composed of detrital limestone (packstone-grainstone-rudstone) and microbial boundstone, with only locally marked lamination. Boundstone, situated about 0.5 m below base of laminated limestone, contains horizon with numerous flat-bottomed caverns (arrows). Location of most samples, subjected to geochemical and isotopic studies is indicated. Samples C, D, E, and F, location of which is not included in photograph, were collected from microbialites in boundstone, occurring 1–1.5 m below base of microbial laminites from the top of exposure

Fig. 5. Boundstone, locally packstone-grainstone, about 0.5 m below base of laminated limestone from top part of exposure. Numerous caverns with flat bottoms developed on laminated microbialites. Limestone contains numerous, calcified, siliceous Lithistida sponges (arrows). Packstone-grainstone visible at bottom left

microbial laminae, separated by coprolitic grainstone, was identified. From these laminae, material for geochemical (5 samples) and isotopic $\delta^{13}C$ and $\delta^{18}O$ studies (13 samples) was then sampled using an engraving device. Geochemical and isotopic studies (respectively 2 and 7 samples) were also conducted on microbialites, obtained from the lower part of the section.

Geochemical investigations were performed at the Activation Laboratory in Ancaster (Canada). Samples were prepared and analysed in a batch system. Each batch contained a method reagent blank, certified reference material, and 17% replicates. Samples were mixed with a flux of lithium metaborate and lithium tetraborate and fused in an induction furnace. The molten melt was poured immediately into a solution of 5% nitric acid containing an internal standard, and mixed continuously until completely dissolved. The samples were run for major oxides and selected trace elements on a combination simultaneous/sequential Thermo Jarrell-Ash ENVIRO II ICP.

Isotopic analyses were performed at the Mass Spectrometry Laboratory at the AGH University of Science and Technology, using a Finningan Delta S Mass Spectrometer. Coprolites from the coprolitic grainstone were analysed under scanning electron microscope. SEM observations were performed at the AGH University of Science and Technology, using a FEI Quanta 200 FEG scanning microscope.

The terminology, used in this paper for the description of microbialites is based on that in papers by Schmid (1996) and Riding (1999, 2000). In the description of stromatolites, the term "micropeloidal stromatolite" is used in relation to stromatolites, bearing micropeloids up to 0.05 mm in diameter (cf. Monty, 1967; Gaillard, 1983; Dromart *et al.*, 1994; Reitner and Schumann-Kindel, 1997; Reolid *et al.*, 2005; Matyszkiewicz *et al.*, 2012). The terminology, applied to the description of carbonate buildups was adapted from Riding (2002).

DESCRIPTION OF EXPOSURE

The steep, rocky slope of the Zegarowe Crags exposes a more than 50-m-long, geological section, which was described in detail by Matyszkiewicz *et al.* (2004, 2006a). The uppermost part of the biohermal complex of the Zegarowe Crags, about 1.5 m thick, is made up of massive limestones, the top of which is consists of about 10 cm of massive, hard limestone showing distinct lamination (Fig. 4). This is a microbial-sponge, agglutinated to open frame reef complex (cf. Riding, 2002). The massive limestone is composed of microbial laminae, ca. 2 mm to 1.5 cm thick, separated by grainstones 1–8 mm thick. Locally, the laminated limestone incorporates, vertical, columnar, microbial structures (Fig. 6F). Microbial laminae of the uppermost part of the laminated limestone locally contain single clasts, up to 1 cm in diameter (Fig. 6B, C). The laminated limestone does not contain any macroscopically visible fauna.

Below the laminated limestone, detrital and locally massive limestone occurs, showing lamination in some parts (Fig. 5). This massive limestone, occurring about 0.5 m below the base of laminated limestone at the top of exposure, includes a horizon about 20 cm thick, with numerous caverns (Figs 4, 5). The caverns are up to about 10 cm in diameter and show flat bottoms, developed on laminated limestone. This part of the section is typified by numerous, macroscopically visible calcified siliceous sponges of the Order Lithistida and thick-shelled gastropods (nerineids; cf. Matyszkiewicz *et al.*, 2004, 2006a).

MICROFACIES ANALYSIS

Sediments below the laminated limestone

The sediments, underlying the laminated limestone (Figs 4, 5), are strongly diversified, both vertically and laterally. They are represented by detrital sediments, mostly grainstones and rudstones (Fig. 6E), subordinately packstones and microbial boundstones (Figs 6D, 7B). In the detrital sediments, there are locally occurring laminae of micropeloidal, peloidal and agglutinated stromatolites, stabilizing the sediment. Boundstone is represented by microbial-sponge associations, where, besides calcified Lithistida sponges, thrombolites and peloidal and agglutinated stromatolites also occur (Fig. 7B). Rudstone (Fig. 6E) comprises irregular intraclasts, up to about 5 mm in diameter, peloids of unknown provenance, and single, indeterminable coprolites, up to 0.9 mm in diameter, with rims of isopachous, granular cement. Some of the intraclasts include partly micritized ooids, up to 0.5 mm in diameter. Apart from the macroscopically identifiable, calcified. siliceous lithistid sponges and gastropods, the fauna contains abundant plates of echinoids (Fig. 6E), as well as micritized benthic and *Crescentiella* sp. foraminifera.

The limestone, showing macroscopically identifiable lamination, is of boundstone and is developed as clotted and laminated thrombolites, micropeloidal, peloidal and agglutinated stromatolites, as well as clotted leiolites (Figs 6D, 7B). Agglutinated stromatolites incorporate single, indeterminable coprolites and fragments of thick-shelled bivalves (Fig. 7B). Clotted thrombolites locally form columnar structures, up to about 1.5 cm high, within which regular and irregular borings were observed (Fig. 6D). Peloidal stromatolites and leiolites incorporate isolated, indeterminable coprolites, up to 1 mm in diameter, usually occurring together with fragments of echinoid plates (Fig. 6D; cf. Matyszkiewicz *et al.*, 2004, 2006a).

In some samples, collected from the strata, underlying the laminated limestone, karst features were observed (?hydrothermal karst *sensu* Wright, 1991), in the form of intensive, metasomatic rock dissolution, recrystallization, and infilling by brown internal sediment of caverns, which are a few millimetres in diameter (Fig. 7B). Stylolites, lined by brown ferric oxides, cut only the unmetasomatosed limestone and do not continue into the metasomatosed limestone (Fig. 7B).

Laminated limestone

The laminated limestone occurring at the top of the Zegarowe Crags section is developed as a boundstone represented by microbial mats, intercalated with laminae of coprolitic grainstone, the dominant component of which is indeterminable, favrenoid coprolites (B. Senowbari-Daryan, pers. comm., 2005).

Microbial laminae are composed of micropeloidal, peloidal and agglutinated stromatolites and subordinately of layered leiolites (Fig. 6A, C). Stromatolites reveal parallel lamination, although local disturbances of lamination also were observed (Fig. 6A). The stromatolites in the uppermost part of the section include poorly rounded clasts of redeposited stromatolites and leiolites, up to about 1 cm in diameter (Fig. 6B, C). Bioclasts comprise only single fragments of thick-shelled bivalves and isolated, thin (up to 5 mm), calcified siliceous sponges of the order Hexactinellida (Fig. 6C).

Coprolitic grainstone (Figs 6F, 7A, 8) occurs between the microbial laminae. The dominant component is micritic coprolites, devoid of distinct microsparitic canals. The coprolites attain 1.2 mm in diameter and are usually coated with rims of isopachous granular cement (Fig. 9). Sporadically, coprolites without cement rims are surrounded by concentrically arranged, micropeloidal packstone (Fig. 8C). At intergranular contacts, isopachous cement rims show a strong reduction in thickness (Figs 7A, 8C). Asymmetrical dissolution textures are common at the basal parts of coprolites, beneath a rim of isopachous granular cement (Figs 6F, 7A, 8, 9; cf. Prezbindowski and Tapp, 1989). These are developed as dissolution pore spaces, within which the infill-

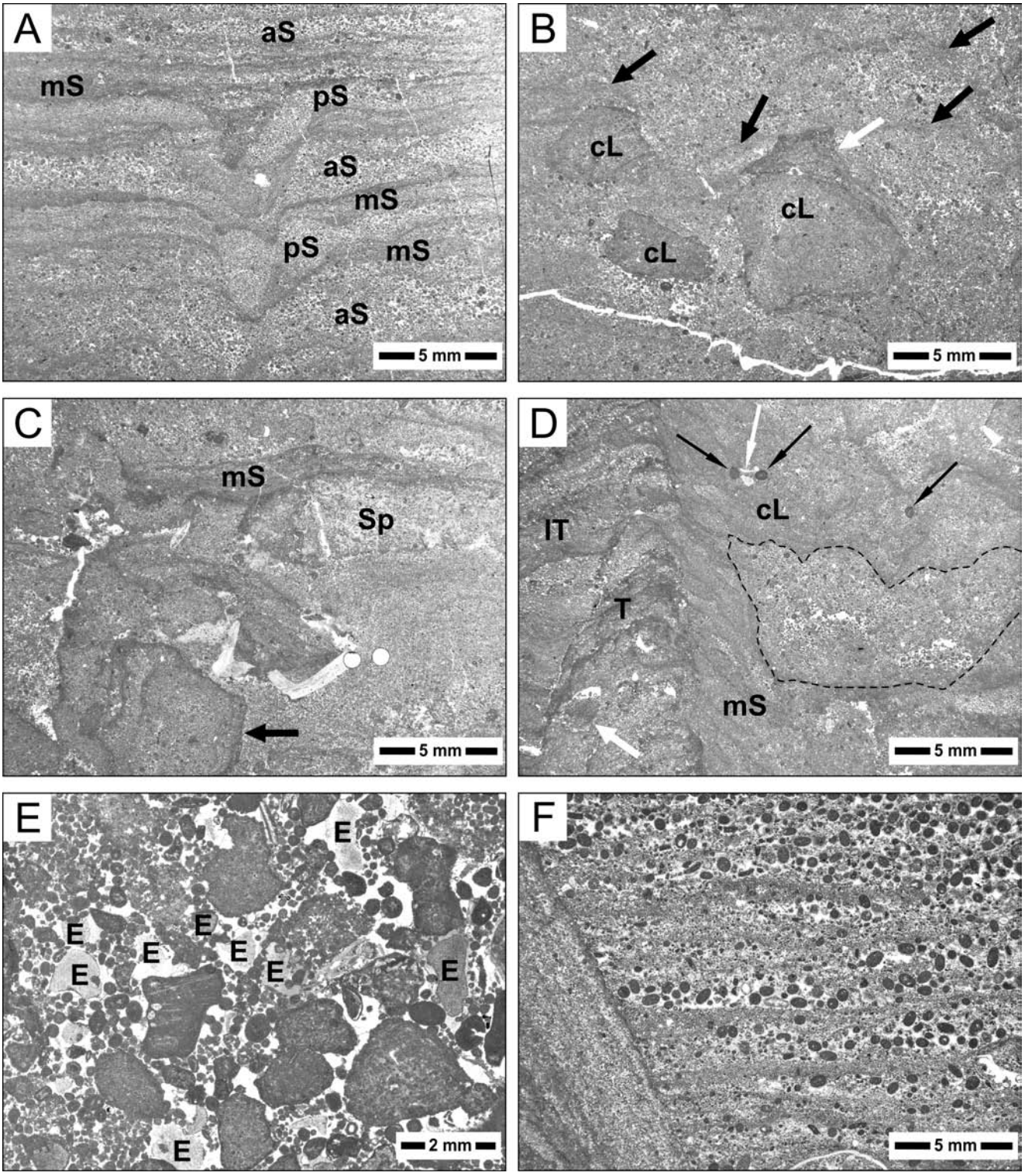

ing sediment was dissolved. Some of the pores are filled with late-diagenetic, granular cement, devoid of micropeloids (Fig. 8D). Locally, fine grains filling in part pore spaces, are coated with bladed cement (Fig. 9B). The coprolites show sometimes compactional deformations (Fig. 8C, D) and, commonly, microborings (Fig. 8D). The microborings are irregular, up to 0.5 mm in diameter, and filled with micropeloidal packstone. In some places, the basal parts of coprolites – beside rims of isopachous cement – are coated with dripstone cement (Fig. 7A), whereas meniscus cement was observed at the contacts between coprolites (Fig. 7A). Both dripstone and meniscus cements occur in those samples where part of the pore space is filled with ferrugineous, vadose crystal silt (Fig. 7A).

Intraclasts, up to 0.6 mm in diameter, are accessory components of the coprolitic grainstone. In the laminated limestone, there also are single, benthic foraminifers, very rare fragments of bivalve shells, and oncoids, up to 0.4 mm

Fig. 6. Microbialites in uppermost part of Zegarowe Crags. **A** – Agglutinating stromatolites (aS), peloidal stromatolites (pS) and micropeloidal stromatolites (mS). Stromatolite laminae are arranged roughly horizontally and parallel to one another, except central part, where disturbance, probably caused by synsedimentary tectonics occurs. Deposition of undisturbed stromatolite laminae visible in upper part post-dated tectonic activity. Laminated limestone; uppermost part of exposure. **B** – Angular, redeposited intraclasts of clotted leiolites (cL) in fine-grained sediment (packstone-wackestone), locally stabilized by laminae of layered leiolites (black arrows). On one of intraclasts, dome-like, layered thrombolite (white arrow) developed after redeposition. Laminated limestone; uppermost part of exposure. **C** – Intraclasts of redeposited microbialites and calcified, siliceous hexactinellid sponge (Sp) in fine-grained sediment (wackestone-packstone), stabilized by micropeloidal stromatolite (mS). In lower part, a poorly rounded intraclast (arrow) composed of micropeloidal stromatolite and clotted leiolite, is visible. In centre, microbial intraclast with right and left boundaries at the bottom marked by bivalve fragments. Laminated limestone; uppermost part of exposure. **D** – On left, columnar thrombolite (T) with oval boring (thick white arrow), passing laterally to left into layered thrombolite (lT), and to right into micropeloidal stromatolite (mS) and clotted leiolite (cL). Fine-grained sediment, with numerous peloids and micropeloids in central part of photograph (lined) probably represent penetration infill. Clotted leiolites incoroprate isolated coprolites (thin black arrows) and fragments of echinoids (thin white arrow). Boundstone; about 0.8 m below laminated limestone, from uppermost part of exposure. **E** – Grainstone-rudstone about 1 m below base of laminated limestone from top of exposure. Grains <1 mm in diameter are well rounded; they include rare microoncoids. Larger, irregular and usually angular grains represent intraclasts of peloidal stromatolites, micropeloidal stromatolites and clotted leiolites. Worth noting are numerous fragments of echinoids (E), commonly with coating syntaxial cement. **F** – Laminae of coprolitic grainstone, intercalated with micropeloidal stromatolites and peloidal stromatolites. On left, fragment of peloidal thrombolite, representing part of columnar structure, separating laminated limestone. Laminated limestone; uppermost part of exposure

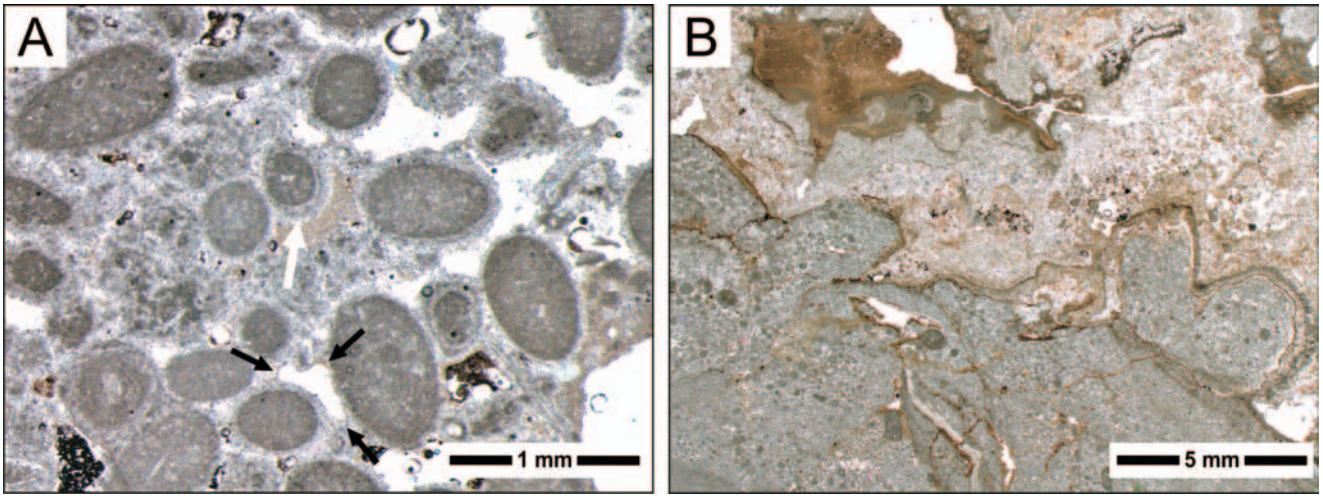

Fig. 7. Vadose cements and metasomatically altered limestones. **A** – Coprolitic grainstone. Porous zone, probably altered in vadose conditions. Some grains, apart from rims of isopachous cement, are coated with dripstone cement (white arrow), showing increased thickness of cement crust in basal parts of coprolites. Meniscus cement (black arrows) occurs at intergranular contacts. Some of pores are filled with ferruginous, vadose crystal silt (occurring below dripstone cement). Laminated limestone, uppermost part of the exposure. **B** – Lower part shows agglutinating and peloidal stromatolites, with isolated, larger intraclasts. Upper part whit metasomatically altered limestone, in which small cavern is filled with brown internal sediment, likely to be associated with hydrothermal karst. Agglutinating and peloidal stromatolites are cut by numerous stylolites, lined with iron oxides, which do not continue into metasomatically altered limestone. Boundstone, about 1.5 m below base of laminated limestone at the top of exposure

in diameter and bearing cortex rims composed of *Girvanella* sp. algae (cf. Matyszkiewicz *et al.*, 2004, 2006a).

CHEMICAL COMPOSITION OF MICROBIALITES

The results of chemical analyses are shown in Table 1. Agglutinating and peloidal stromatolites from the laminated limestone of the uppermost part of the section are typified by considerable stability of chemical composition. This composition approaches that of stromatolites with similar characteristic and comparable stratigraphic position, recently described by Matyszkiewicz *et al.* (2012) from agglutinated, microbial to open frame reefs at Czajowice, in the southern part of the Kraków–Częstochowa Upland. The latter are interpreted as the deposits of a high-energy environment with a low rate of sedimentation and poor nutrient availability.

Two samples (C and F), collected from the strata that underly the laminated limestone, show minor differences in chemical composition. Sample C, showing microscopically distinct, metasomatic alterations (Fig. 7B), has increased amount of SiO_2, Al_2O_3, Fe_2O_3, P_2O_5 as well as Ba and Zn, compared to other samples, and a concomitant decrease in the amounts of MnO, MgO, CaO and Sr. Sample F exhibits an increased amount of Zn.

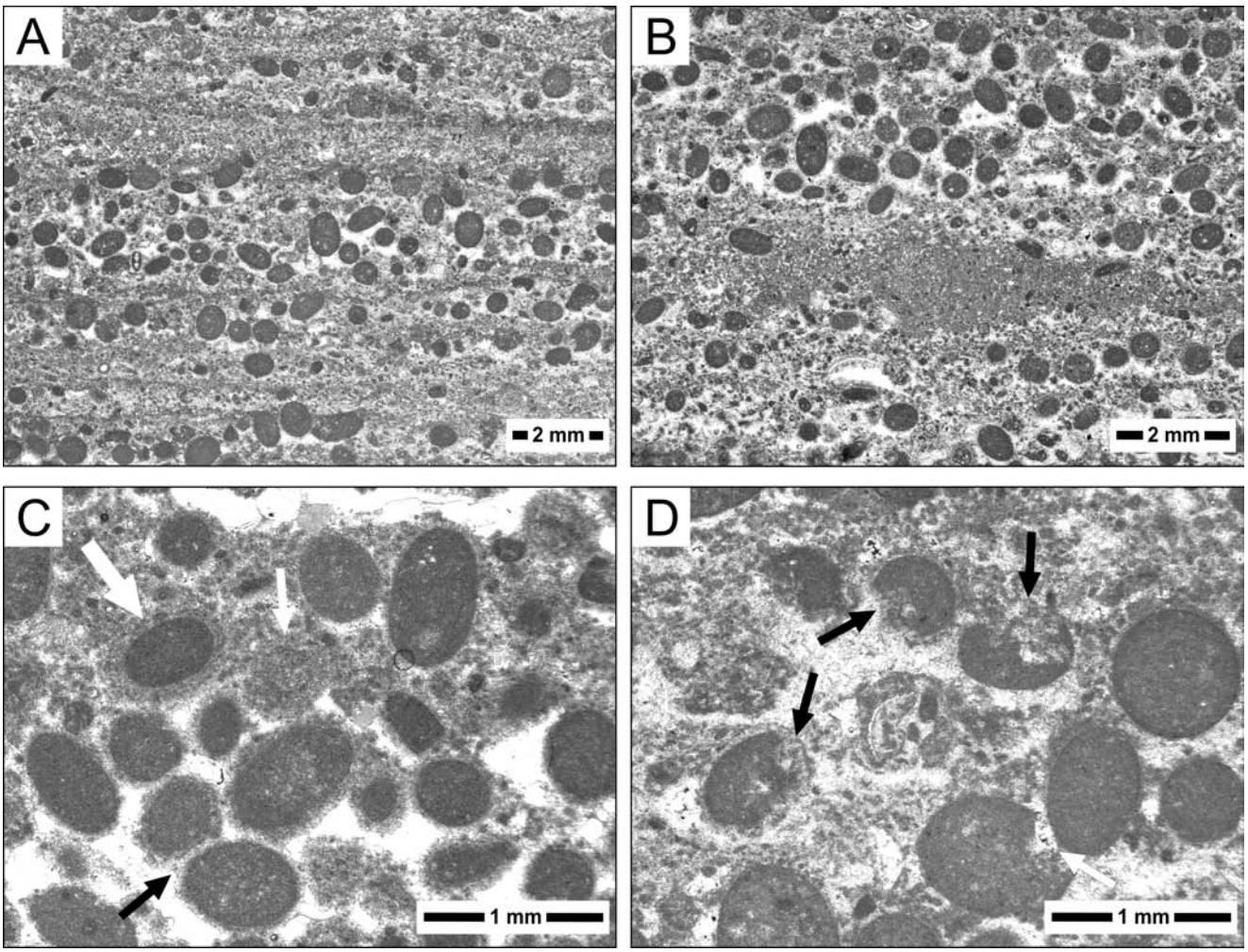

Fig. 8. Microfacies with coprolites in uppermost part of Zegarowe Crags. **A** – Coprolitic grainstone and micropeloidal stromatolite. Coprolitic grainstone show high porosity, usually developed at base of coprolites (asymmetric dissolution textures). Laminated limestone; uppermost part of exposure. **B** – Coprolitic grainstone. Wackestone, separating coprolite-bearing laminae, is fine-grained sediment, originating in absence of microbialites. Laminated limestone; uppermost part of exposure. **C** – Coprolitic grainstone. Coprolites are typically bounded by a rim of isopachous cement, which is usually thicker in basal parts of coprolites. Sporadically, coprolites devoid of cement rims are coated by concentrically developed micropeloidal packstone (big white arrow). To right of coprolite with micropeloidal packstone rim, microcoprolites form an oval aggregate of diameter approaching that of coprolites (small white arrow). Coprolites, devoid of isopachous cement rim, rarely show compactional deformations (black arrow). Laminated limestone; uppermost part of exposure. **D** – Coprolitic grainstone. Upper parts of coprolites are surrounded by matrix with numerous micropeloids. Pore spaces, developed below base of coprolites, is filled with granular cement, which is devoid of micropeloids. Compactional deformation of one of coprolites visible on lower right (white arrow). Some of coprolites show distinct traces of microborings (black arrows), filled with micropeloidal packstone. Laminated limestone, uppermost part of exposure

Table 1

Major elements of microbialites from Zegarowe Crags

Sample	Stromatolite type	SiO_2 (%)	Al_2O_3 (%)	Fe_2O_3 (%)	MnO (%)	MgO (%)	CaO (%)	Na_2O (%)	K_2O (%)	TiO_2 (%)	P_2O_5 (%)	L.O.I. (%)	Total (%)	Ba (ppm)	Sr (ppm)	Zn (ppm)
Sm1-1*	agglutinating	0.18	0.01	0.03	0.013	0.31	55.50	<0.01	0.01	<0.001	0.03	43.86	99.93	15	118	15
Sm1-2*	peloidal	0.13	0.06	0.03	0.018	0.30	56.12	0.01	<0.01	<0.001	0.04	43.85	100.54	4	114	13
Sm1-3*	agglutinating	0.12	0.04	0.06	0.014	0.30	55.88	0.04	0.03	<0.001	0.04	43.82	100.35	4	115	11
Sm1-4*	agglutinating	0.11	0.05	0.06	0.020	0.29	56.08	0.04	<0.01	<0.001	0.05	43.81	100.50	3	113	11
Sm2-6*	micropeloidal	0.16	0.08	0.03	0.014	0.31	56.32	0.04	0.05	<0.001	0.07	43.43	100.50	4	120	15
C**	agglutinating	0.97	0.20	0.33	0.009	0.19	54.81	0.04	0.06	<0.001	0.36	43.26	100.23	24	84	44
F**	peloidal	0.20	0.08	0.06	0.011	0.33	56.07	0.04	0.05	<0.001	0.10	43.65	100.59	11	122	50

* localization of sample in given in the Fig. 4; ** sample represents microbialites occurring ca. 1.2 m below the base of microbial laminites from the top of exposure

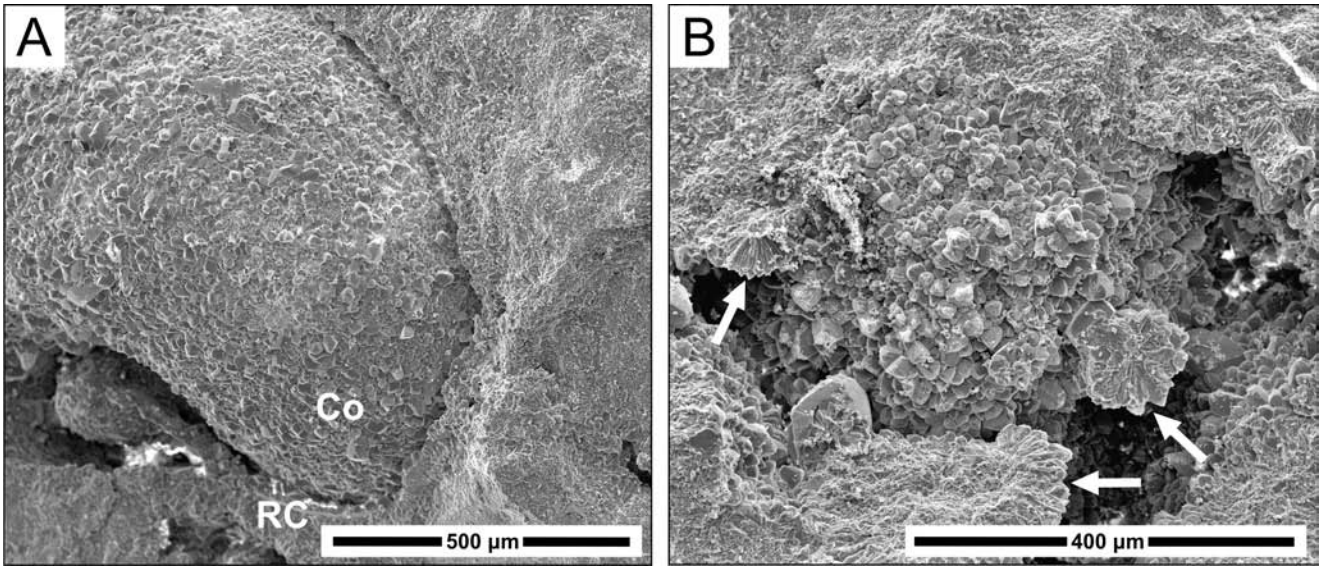

Fig. 9. SEM photomicrographs of cements covering coprolites and infilling the porous space. **A** – Lower part of coprolite (Co; centre and left) with a cover of isopachous rim cement (RC), developed as closely spaced rhombohedral crystals. Open space between coprolite and rock matrix is interpreted as asymmetrical dissolution texture. Coprolitic grainstone. SEM image. **B** – Cements, filling pore space beneath coprolite. In central part, rhombohedral crystals of isopachous cement developed at base of coprolite are visible. Small grains, filling in part pore space are coated by thin fringes of bladed cement (arrows), which increase in width along their length. Coprolitic grainstone. SEM image

ISOTOPIC ANALYSIS

Three groups of samples: Sm1, Sm2 and A, form a pattern of $\delta^{13}C$ values falling into a very narrow interval between +2.4 and +2.7‰ (Fig. 10A). This indicates stability of carbon flux in the solution (amount of dissolved carbon and its origin), as well as constant. physico-chemical conditions of carbonate precipitation. The oxygen isotopic composition in these groups shows a greater variability: from –2.1‰ to –0.9‰. Two Sm3 samples and samples C, D, E and F show greater differentiation in isotopic composition.

The oxygen isotopic composition in precipitated carbonates was mainly controlled by isotopic composition of the water and by temperature. Under conditions of isotopic equilibrium, all these of parameters can be described by the formula of O'Neil *et al.* (1969):

$$1000 \ln \alpha_{C\text{-}W} = \frac{2.78 \cdot 10^6}{T^2} - 2.89 \qquad (1)$$

where: T is absolute temperature, $\alpha_{C\text{-}W}$ is the equivalent coefficient of oxygen isotope fractionation between calcite and water, expressed as:

$$\alpha_{C\text{-}W} = \frac{1000 + {}^{18}O_{CaCO_3}}{1000 + {}^{18}O_{H_2O}} \qquad (2)$$

in which $\delta^{18}O_{CaCO_3}$ and $\delta^{18}O_{H_2O}$ describe oxygen isotopic composition in calcite and water, respectively.

Correct determination of palaeotemperatures basing on equations (1) and (2) requires knowledge of the isotopic composition of water. Moreover, it has to be assumed that, during calcite precipitation, there were no kinetic effects usually related to rapid degassing of solution or water evaporation. The first ones led to underestimation, the second ones – to overestimation of palaeotemperatures accompanying carbonate precipitation. In the case of examined samples, none of these conditions of palaeotemperature determination could be verified experimentally. The results of calculations basing on presented relationships for the two isotopic compositions of water, namely: 0‰, reflecting present-day composition of sea water, and –2‰, reflecting isotopic composition of waters of warm climate and showing a minor admixture of continental water, are listed in Table 2.

Figure 10B shows oxygen isotope composition within calcite precipitated under conditions of isotopic equilibrium as a function of temperature, calculated for two values of $\delta^{18}O$ in water. Isotopic composition of the examined samples is also shown. If carbonates precipitated from sea water in equilibrium conditions, then the temperature interval for most of the samples would be between 20 and 25 °C. Higher temperatures typify samples Sm3-2, F and C, with the last sample showing the highest value of 36.6 °C (Fig. 10B).

Palaeotemperatures calculated at a slightly lower, isotopic composition of water, with $\delta^{18}O$ equal to –2‰, are lower than the quoted ones by about 8–9 °C. This second scenario reflects a situation of carbonates supplied by continental waters, the isotopic composition of which should not be negative to a significant extent. If the time remaining up to carbonate precipitation is not too long, then the carbonates will not manage to balance their oxygen isotopic composition with respect to sea water.

On the basis of the calculated temperatures, one can estimate the isotopic composition of carbon in its gaseous phase, controlling the composition of dissolved carbonates in open systems. The relationship between the isotopic composition of carbon in calcite and gaseous carbon dioxide can be presented (Deines *et al.*, 1974) as:

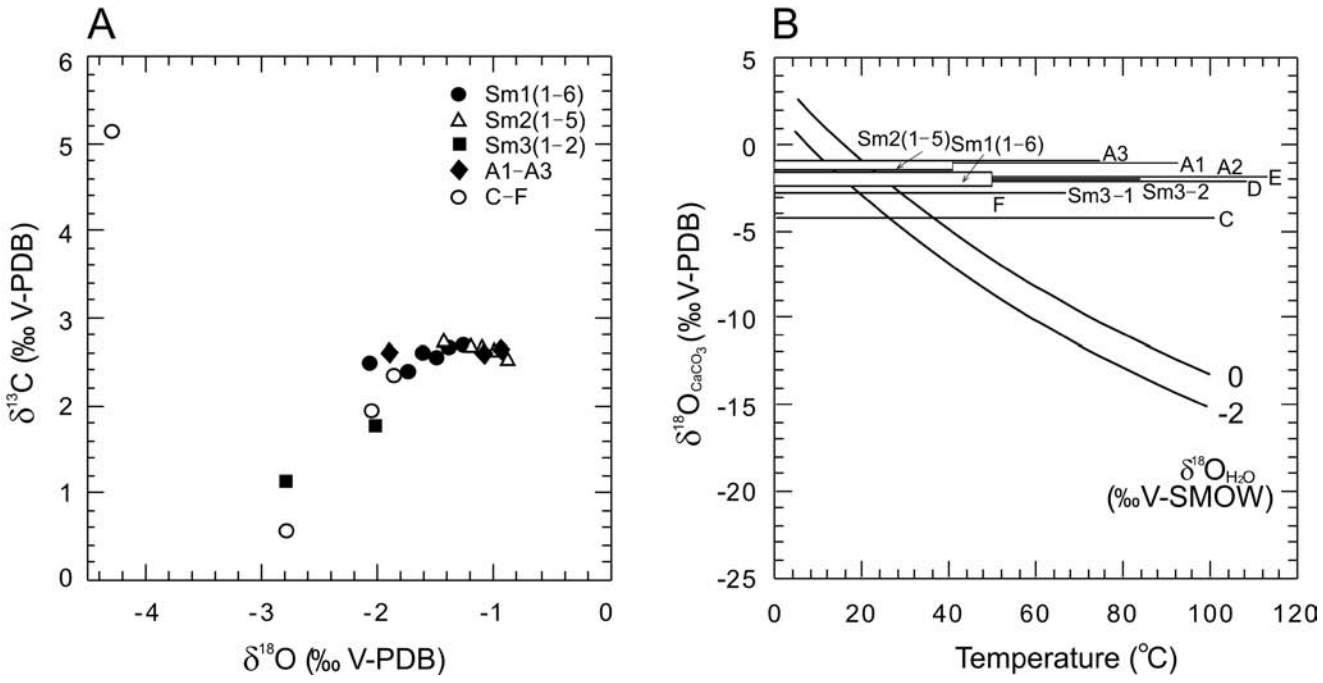

Fig. 10. Results of isotopic analyses and their interpretation. **A** – Diagram, showing results of isotopic analyses. **B** – Oxygen isotope composition within calcite, precipitated under conditions of isotopic equilibrium, as a function of temperature for the values of $\delta^{18}O$ = 0‰, equivalent to composition of contemporary sea water, and $\delta^{18}O$ = –2‰, equivalent to composition of warm-climate sea water, with a minor admixture of terrestrial water. Isotopic composition of samples studied is shown as well

$$1000 \ln \alpha_{CaCO_3\text{-}CO_2(g)} \quad \frac{1.19 \cdot 10^6}{T^2} - 3.60 \qquad (3)$$

where: T is absolute temperature, $\alpha_{CaCO_3\text{-}CO_2(g)}$ is the equivalent coefficient of carbon isotope fractionation between calcite and gaseous CO_2, expressed by:

$$\alpha_{CaCO_3\text{-}CO_2(g)} \quad \frac{1000 + {}^{13}C_{CaCO_3}}{1000 + {}^{13}C_{CO_2(g)}} \qquad (4)$$

Results of calculations using equations (3) and (4) are listed in Table 2.

DISCUSSION

Palaeoenvironmental interpretation of depositional setting

The Late Jurassic sedimentary environment of Zegarowe Crags complex was situated on a shallow shelf near the storm wave base within the euphotic zone. The term 'shallow' has been taken to refer to locations down to 30 meters. The shallow-water character of the environment and higher water energy is indicated by the presence of *Girvanella* sp. algae, cross-stratification in the grainstones interbedded with the microbialites, and stratiform, peloidal and agglutinating stromatolites (cf. Matyszkiewicz *et al.*, 2006a, 2012). Stromatolites are a product of microbially induced or microbially influenced mineralization (Dupraz *et al.*, 2009). Development of the stromatolites proceeded mainly at low sedimentation rates (cf. Keupp *et al.*, 1993; Dupraz and Strasser, 1999; Olivier *et al.*, 2003, 2010; Reolid, 2011; Matyszkiewicz *et al.*, 2012). Peloids and micropeloids building the stromatolites were precipitated within an active biofilm, which developed on laminae of coprolitic grainstone, rich in organic compounds. It is likely that the formation of stromatolites was controlled by the fine nutrient content of the suspension in waters and the high energy of the sedimentary environment. Under conditions of early diagenesis, a rearrangement of acid macromolecules in the microbial biofilm took place, providing an organized nucleation template for pervasive biofilm organomineralization (cf. Reitner, 1994; Neuweiler *et al.*, 1999, 2000; Decho, 2000). This biofilm certainly also surrounded single coprolites, as indicated by the presence of micropeloidal packstone, developed concentrically upon the coprolites without cement rims.

Most of the isotopic compositions of gaseous CO_2, calculated assuming temperatures resulting from $\delta^{18}O_{H_2O}$ = 0‰, range between –7.2‰ and –7.6‰. These figures approach those of atmospheric carbon dioxide from before the industrial era. Acceptance of temperatures resulting from the assumption of $\delta^{18}O_{H_2O}$ = –2‰, leads to values about 0.8‰ lower, which may have resulted from a very small admixture of biogenic CO_2. Sample C shows the highest values, about 4‰. The measured values of $\delta^{18}O_{CaCO_3}$ and $\delta^{13}C_{CaCO_3}$ indicate that precipitation of the carbonates proceeded in shallow-water conditions and in climate resembling the present-day one. The shallow depths of the basin are indicated by the calculated $\delta^{13}C_{CO_2(g)}$ values, which indicate the dominant role of atmospheric CO_2 in controlling the isotopic composition of the carbon, dissolved in the water.

Table 2

Results of isotopic analyses of microbialites from Zegarowe Crags

Sample	Type of stromatolite	$\delta^{18}O$ (‰ V-PDB)	$\delta^{13}C$ (‰ V-PDB)	Paleotemperature 1 † (°C)	Paleotemperature 2 ‡ (°C)	$\delta^{13}C_{CO_2(g)}$ 1 § (‰ V-PDB)	$\delta^{13}C_{CO_2(g)}$ 2 # (‰ V-PDB)
Sm1-1*	agglutinating	–1.40	2.67	22.1	13.3	–7.4	–8.2
Sm1-2*	peloidal	–2.09	2.50	25.4	16.2	–7.2	–8.1
Sm1-3*	agglutinating	–1.27	2.70	21.5	12.7	–7.4	–8.2
Sm1-4*	agglutinating	–1.62	2.60	23.2	14.2	–7.3	–8.2
Sm1-5*	peloidal	–1.75	2.40	23.8	14.8	–7.5	–8.3
Sm1-6*	micropeloidal	–1.51	2.56	22.7	13.7	–7.4	–8.3
Sm2-1*	agglutinating	–1.21	2.67	21.3	12.5	–7.4	–8.3
Sm2-2*	peloidal	–1.03	2.64	20.4	11.7	–7.5	–8.4
Sm2-3*	agglutinating	–1.44	2.74	22.3	13.5	–7.3	–8.1
Sm2-4*	peloidal	–1.12	2.67	20.9	12.1	–7.5	–8.3
Sm2-5*	peloidal	–0.90	2.53	19.8	11.2	–7.7	–8.6
Sm3-1*	agglutinating	–2.80	1.13	28.8	19.4	–8.3	–9.1
Sm3-2*	peloidal	–2.02	1.78	25.1	15.9	–8.0	–8.8
A1*	peloidal	–0.97	2.64	20.2	11.5	–7.6	–8.4
A2*	agglutinating	–1.91	2.61	24.5	15.4	–7.2	–8.0
A3*	agglutinating	–1.10	2.63	20.8	12.0	–7.5	–8.4
C**	agglutinating	–4.30	5.15	36.6	26.4	–3.7	–4.5
D**	agglutinating	–2.07	1.96	25.3	16.2	–7.8	–8.6
E**	peloidal	–1.87	2.36	24.3	15.3	–7.5	–8.3
F**	peloidal	–2.80	0.59	28.8	19.4	–8.8	–9.7

* localization of sample is given in the Fig. 4; ** sample is collected from microbialites within boundstone occurring 1-1.5 m below the base of microbial laminites from the top of exposure; † calculated assuming $\delta^{18}O_{H_2O} = 0$ (‰ V-SMOW); ‡ calculated assuming $\delta^{18}O_{H_2O} = -2$ (‰ V-SMOW); § calculated assuming palaeotemperature 1; # calculated assuming palaeotemperature 2

Coprolites as an indicator of sedimentary environment

The mass occurrences of coprolites within the coprolitic grainstone of the Zegarowe Crags represent favrenoid coprolites, but their state of preservation precludes precise determination. The form-genus *Favreina* is attributed to the anomuran superfamilies Thalassinoidea and Galatheoidea (Brönnimann, 1972).

The crab fauna of the Upper Jurassic microbial-sponge and microbial facies have been described by numerous authors (i.e., Beurlen, 1928; Barczyk, 1961; Merta, 1972; Nitzopoulos, 1973; Meyer, 1975; Collins and Wierzbowski, 1985; Förster and Matyja, 1986; Müller *et al.*, 2000; Helm, 2005; Krobicki and Zatoń, 2008; Kato *et al.*, 2011; Schweigert and Koppka, 2011), while the coprolites, occurring within such sediments have been reported sporadically and usually as single specimens.

In the Upper Jurassic carbonate buildups, crustacean coprolites are found mainly in coral thrombolite patch reefs, coral biostromes and coral carpets (Schweigert *et al.*, 1997; Helm and Schülke, 2004; Helm, 2005), unequivocally interpreted as originating in shallow-water near-reef environments, lagoons, or specific Solnhofen-type facies (Dietl and Schweigert, 2001; Schweigert, 2010), representing isolated, inter-reef basins of increased salinity.

Mass occurrences of coprolites are also observed in fissures and caverns, interpreted in some instances as karst features. Accumulations of favrenoid coprolites in agglutinated stromatolites, filling caverns in the so-called, fungiid biostromes, with an abundant fauna of thin platy corals, were reported by Herrmann (1996) from the Upper Jurassic strata of a carbonate platform in Dobrogea (Romania). This author interpreted the sedimentary environment of these sediments as located immediately below the wave base, unlike Draganescu (1976), who postulated an extremely shallow-water intertidal plain. From the Upper Jurassic reefal to lagoonal Ota Limestone, Schweigert *et al.* (1997) described favrenoid coprolites, forming accumulations within open karst fissures. These fissures were subsequently flooded after a rapid sea level rise, favouring inflow of the coprolites.

Gaździcki *et al.* (2000) described *Parafavreina* coprolites from shallow marine, mostly lagoonal facies of the uppermost Triassic (Norovica Formation; Western Carpathians). They occur in laminated oobiopelsparites (Gaździcki *et al.*, 2000, plate I, p. 247), very much like the laminated limestones at the Zegarowe Crags.

Coprolites are also known from deeper-water environments, where their occurrence is frequently associated with the presence of hydrocarbon-seeps or hydrothermal vents. Gaillard *et al.* (1985, 1992) have described coprolites, occurring in Oxfordian 'pseudobioherms' in the Beauvoisin (Drôme) region in SE France, in the Terres Noires Formation. These deposits originated close to active synsedimentary faults, at hydrocarbon seeps in the central part of a deep-sea basin, undergoing subsidence. The deposits comprise indeterminable coprolites (Fig. 6D; Gaillard *et al.*,

1992, p. 456), the characteristics of which resemble those described from the Zegarowe Crags. There are similarities in both the size of the coprolites and their mass occurrence, as well as the presence of meniscus cement, developed on inter-coprolite contacts and interpreted as being a result of precipitation from solutions, which removed part of the fine-grained matrix. Senowbari-Daryan *et al.* (2007) have documented crustacean coprolites from the Beauvoisin region, the abundance of which at seeps is interpreted as being function of nutrient availability.

Schweigert *et al.* (1997) described Favrenidea coprolites from the condensed, Middle Jurassic, pelagic deposits of the External Subbetics of Southern Spain. Densely packed coprolites occur within lenses as the only bioclasts and are extensively replaced by goethite and hematite. Some of these coprolites are strongly compacted, preventing their determination.

The presence of numerous, well-preserved, crustacean coprolites cf. *Favreina* sp. was confirmed by Lehmann (2007) within a calcite vein, determined to be Hauterivian–Valanginian, in a ponded basalt flow at the bottom of Site 304 (Deep Sea Drilling Project, Leg 32; NW Pacific). Figures attached to the paper quoted show coprolites with asymmetric dissolution textures, as well as meniscus and dripstone cements (Lehmann, 2007, pl. 2, p. 833).

Buchs *et al.* (2009) described crustacean coprolites from a 200-m-thick Palaeocene sequence in Southern Costa Rica, largely dominated by pillow lavas and interpreted as originating in deep-water conditions. Coprolites occur there in hydrothermally altered interpillow sediments, fragmented during hydrothermal processes, and in places are slightly deformed by mechanical compaction. The morphology of these coprolites indicates that they have not been transported over long distances before being deposited in caverns between the pillow lavas. Buchs *et al.* (2009) concluded that the coprolites were fed by chemosynthetic bacteria, which developed owing to hydrothermal activity related to volcanism.

Kietzmann *et al.* (2010) described Middle Tithonian–Lower Valanginian crustacean microcoprolites from the Neuquèn Basin, Argentina. These coprolites occur in laminated packstones and grainstones, which were interpreted as middle ramp to basin sediments. Bujtor (2012) and Jáger *et al.* (2012) documented in the Mecsek Mts. (Hungary) Valanginian crustacean microcoprolites from shallow-marine, hydrothermal vents, which could have contributed to the creation of favourable temperature or nutritional conditions for decapod crustaceans. In partly metasomatosed limestone, crustacean microcoprolites represent the only microfaunal element.

It follows from the above examples that one of main criteria controlling the occurrence of an abundant, coprolite-producing crab fauna, is periodic nutrient availability. The latter can be controlled by a variety of factors, including hydrothermal vents and active synsedimentary tectonics. Jeng *et al.* (2004) described from the contemporary, shallow shelf of Taiwan the unusual activity of crabs *Xenograpsus testudinatus*, associated with hydrothermal vents. During increased hydrothermal activity, the sea water shows a high concentration of inorganic particles and dead or narcotized zooplankton, which are food for the crabs. In periods of low, hydrothermal activity or its absence, the lack of nutrients causes the crabs to return to their crevices. Dando *et al.* (1995) related activation of hydrothermal venting to earthquakes in the Hellenic volcanic island arc, documenting as well coeval enrichment of sea water with phosphate. The presence of phosphate in an oligothrophic sea could be an important factor, determining the development of zooplankton.

The lack of preservation in the coprolites of microsparitic canals, the infill of which would permit the determination of ichnospecies, is problematical. The canals are formed by pyloric fingerlets inside the crustacean's gut (Powell, 1974). Kietzmann *et al.* (2010) assume that the lack of canal preservation probably could be a consequence of both the higher availability of mud and compaction. Schweigert *et al.* (1997, p. 61) also highlight compaction as a factor, making the determination of some of coprolites difficult.

The coprolites from the Zegarowe Crags rarely display compactional deformations. The lack or poor development of microsparitic canals appears to be associated with the strong activity of a live, bacterial biofilm, in which intensive micritization processes were taking place. The presence of isopachous, granular cement rims on the coprolites indicates that the majority of coprolites were deposited as already largely lithified grains. Moreover, in a shallow-water environment of low sedimentation rate, documented by the presence of agglutinating and peloidal stromatolites (cf. Matyszkiewicz *et al.*, 2012), complete lithification of the coprolites proceeded much earlier than the deposition of sediment, of sufficient thickness for the development of mechanical compaction (cf. Kochman, 2010).

Analysis of fauna in section examined

The faunal communities associated with modern hydrothermal vents, are dominated mainly by tube worms, crabs, gastropods, and agglutinated foraminifera. From these settings echinoids and holothurians also have been described, in association with microbial mats (Sudarikov and Galkin, 1995; Van Dover, 1995; Jach and Dudek, 2005). According to Dando (2010), at shallow depths vent-obligate taxa are absent.

Calcified, siliceous sponges are the only more numerous, faunal components of the section examined. The remaining fauna, namely: thick-shelled gastropods, bivalves and ostracods, although present, represent accessory components. The lower part of the Zegarowe Crags section, not described in this paper, is dominated by Hexactinellida (cf. Matyszkiewicz *et al.*, 2004, 2006a), and in the top part the amount of Lithistida increases markedly. Only the uppermost part of the section, developed as micropeloidal, peloidal and agglutinated stromatolites with redeposited clasts devoid of coprolites, includes extremely rare and thin (up to 5 mm) hexactinellid, siliceous sponges.

The observed trend appears to be related to the type of nutrient components. While hexactinellida sponges feed on dissolved amino acids and colloidal, organic matter, lithistida sponges prefer nutrients in the form of particulate, organic matter (Krautter, 1998; Reolid, 2011). However, it is

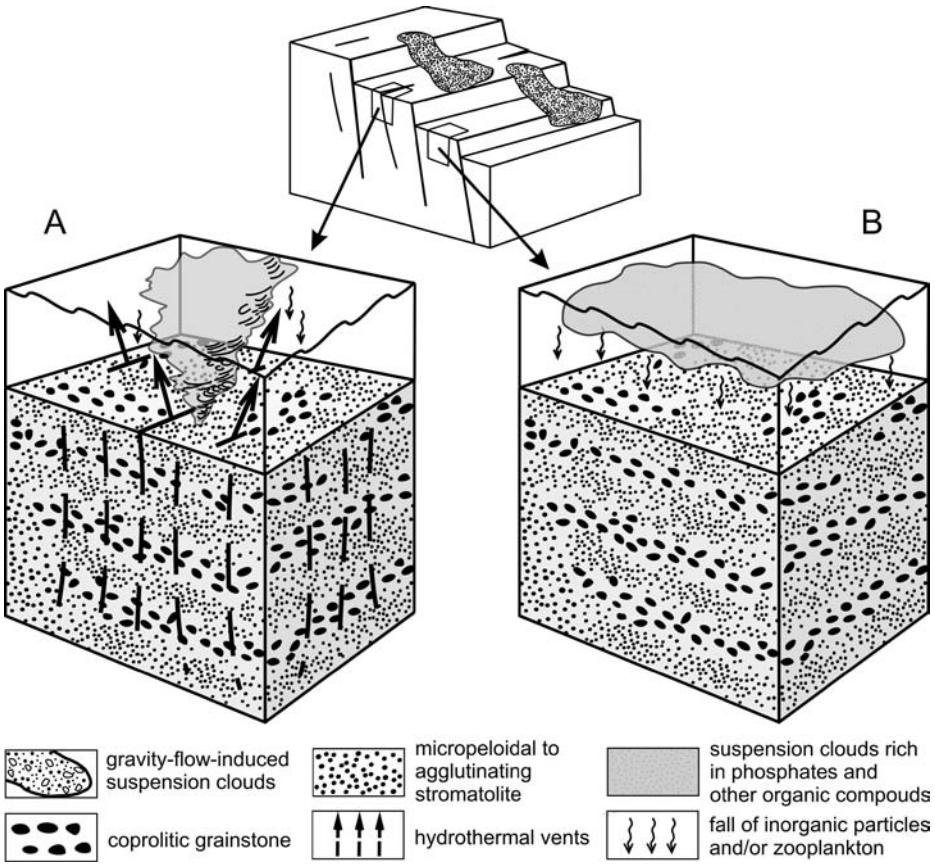

Fig. 11. Two scenarios, proposed to explain origin of grainstone laminae, rich in coprolites. Zegarowe Crags region is situated in area affected by Late Jurassic, active, synsedimentary fault tectonics. Crabs, producing coprolites, developed in conditions of periodic nutrient abundance, which could have been associated with (**A**) activity of low-temperature, hydrothermal vents, related to periodic reactivation of fault tectonics. Periodic, toxic, hydrothermal vents could have resulted in occurrence of high concentration of inorganic particles and dead or narcotized zooplankton as food for crabs. Results of geochemical and especially isotopic analysis do not record, however, influence of hydrothermal fluids on microbial laminae. In another scenario (**B**), development of laminae with coprolites could have been related only with active synsedimentary tectonics, which – leading to formation of gravity flows – produced periodically occurring suspension clouds, rich in phosphates and other organic compounds. Presence of such substances contributed to intensive development of zooplankton as food for crabs

likely, that nutrient availability in the Late Jurassic basin of the northern margin of the Tethys was mainly controlled by local, sedimentary conditions, and not by regional features (Matyszkiewicz *et al.*, 2012). Nutrients, in the form of particulate, organic matter, were supplied to the lower parts of sea bottom or dominated in periods of aggradational growth, when intensive development of benthic organisms took place. In Late Oxfordian time, the Zegarowe Crags formed a distinct elevation on the sea bottom where, oligotrophic conditions, typified by minor amount of nutrients, might be expected to have occurred. Such conditions probably favoured the development of stromatolites, accompanied by a simultaneous, significant reduction in the numbers of siliceous sponges, particularly Lithistida (cf. Matyszkiewicz *et al.*, 2012). However, Lithistida occurring in the top part of the section, indicates point to the presence of nutrients, in the form of particulate, organic matter.

Possible occurrence of hydrothermal karst

The Zegarowe Crags section exhibits structures, which can be related to hydrothermal karst (*sensu* Wright, 1991), including: asymmetrical dissolution textures (cf. Prezbindowski and Tapp, 1989), developed at the basal parts of coprolites (Figs 6F, 7A, 8, 9,), meniscus and gravitational cements in the coprolitic grainstone (Figs 7A, 8C), metasomatosed parts of microbial boundstone with internal sediments (Fig. 7), and increased Zn content in some samples. Most of these features can be explained by the hydrodynamic activity of thermal solutions, circulating within the sediment and removing part of fine-grained matrix (cf. Gaillard *et al.*, 1992). Hydrothermal, karst-related dissolution probably resulted also in the presence of numerous, flat-bottomed caverns in the microbial laminites (Figs 4, 5).

It is not clear, whether during the development of the Zegarowe Crags complex there was active hydrothermal activity, in the form of hydrothermal vents related to the Late Jurassic active synsedimentary tectonics (Fig. 11). The results of geochemical studies do not exclude the possibility of a weak influence of hydrothermal solutions upon the deposited sediment, leaving unsolved the question of the timing of such phenomena (cf. Szulc *et al.*, 2006). There is no doubt that fluids, mineralizing Upper Jurassic deposits, were supplied, at least in part, along stylolites (Fig. 7B),

which originated under the burden of a few hundred metres of rock, that was certainly later than in Late Jurassic time. Increased Zn content, in turn, does not exclude the possibility of genetic relationship between of this mineralization and one of several phases of Zn-Pb deposit formation in the Silesian-Kraków homocline (Bednarek *et al.*, 1985; Jacher-Śliwczyńska and Schneider, 2004; Pulina *et al.*, 2005). Undoubtedly, some faults could have acted as fluid pathways (cf. Sibson, 1987; Aranburu *et al.*, 2002). This particularly relates to carbonate platforms underlain by intrusions, the cooling of which lasted a long time and was associated with several episodes of subsequent activity (Morad, 1998).

The results of isotopic analyses do not reflect any influence of hydrothermal fluids on the deposited sediment. Even if Late Jurassic, hydrothermal vents were present at the time of deposition, the isotopic record would have marked such an activity only during rapid deposition. However, carbonates, transported by thermal waters, might have had enough time to counterbalance their isotopic composition with that of sea water; the amount of them was not enough so as to modify considerably the isotopic composition of sea water in a vast, relatively shallow basin. In this case, the isotopic composition of carbonates would have reflected the conditions, prevailing in the sea water, even when the dissolved carbon would have been supplied to the place of deposition in thermal waters. The observed, minor scatter of $\delta^{18}O_{CaCO_3}$ and $\delta^{13}C_{CaCO_3}$ values (perhaps except sample C) could be a result of a variable depth of precipitation.

CONCLUSIONS

The deposition of microbial laminites, occurring at the top of the Zegarowe Crags took place in a shallow sea, in waters with a chemical composition, resembling the present-day one, in well oxygenated conditions, controlled by the influx of waters enriched in nutrients, the energy of the sedimentary environment and the sedimentation rate. The structure of stromatolites, which predominate in the laminated limestone of the Zegarowe Crags, indicates a low sedimentation rate and low nutrient availability. A low sedimentation rate also is evidenced by the ubiquitous presence of microborings in coprolites, which are filled with micropeloidal packstone of microbial origin.

Disturbances in the stromatolite laminae can be related to the presence of numerous Upper Jurassic gravity-flow deposits in the marginal parts of the Smoleń horst. They indicate active, synsedimentary tectonics during the development of the complex of carbonate buildups. The presence of redeposited clasts in the laminated microbialites is associated with synsedimentary tectonics or represents the effects of the wave base, because of a considerable shallowing during progradation of the complex of carbonate buildups.

The mass occurrence of crab coprolites was an effect of a notable increase in nutrient availability in the sea water. The increasing nutrient availability may have resulted from the development of clouds of suspended, fine-grained sediment. This probably was an effect of synsedimentary tectonics, likely to have been associated with hydrothermal vents. However, the results of geochemical and isotopic studies do not confirm any influence of hydrothermal vents, in the Late Oxfordian, in the area of the Zegarowe Crags complex. It is likely that synsedimentary tectonics alone would have favoured the occurrence in sea water of abundant, nutrient-rich suspensions, related to tectonically activated, submarine mass movements.

Acknowledgements

The project was funded by the National Science Centre, on the basis of contract No. DEC-2011/03/B/ST10/06327, and from a statutory grant of the AGH University of Science and Technology. The authors would like to thank B. Senowbari-Daryan for an attempt at determination of coprolites, M. Duliński for isotopic analyses and comments on the interpretation of the results and A. Gaweł for SEM photographs. The paper has benefitted from valuable comments and suggestions by M. Reolid, A. Gaździcki and an anonymous reviewer. We thank especially Editor M. Gradziński for commenting on the manuscript.

REFERENCES

Aranburu, A., Fernández-Mendiola, P. A., López-Horgue, M. A. & García-Mondéjar, J., 2002. Syntectonic hydrothermal calcite in a faulted carbonate platform margin (Albian of Jorrios, northern Spain). *Sedimentology*, 49: 875–890.

Barczyk, W., 1961. Le Jurassique de Sulejów. *Acta Geologica Polonica,* 11: 3–102. [In Polish, French summary].

Bednarek, J., 1974. *Budowa geologiczna strefy wychodni górnojurajskich między Zawierciem, Łazami i Pilicą*. Unpublished PhD. Thesis, Faculty of Geology, Warsaw University, 193 pp. [In Polish].

Bednarek, J., Kaziuk, H. & Zapaśnik, T., 1978. *Objaśnienia do szczegółowej mapy geologicznej Polski 1:50000, arkusz Ogrodzieniec*. Wydawnictwa Geologiczne, Warszawa, 76 pp. [In Polish].

Bednarek, J., Górecka, E. & Zapaśnik, T., 1985. Tectonically controlled development of ore mineralization in Jurassic sequence of the Silesian-Cracovian Monocline. *Annales Societatis Geologorum Poloniae*, 53: 43–62. [In Polish, English summary].

Beurlen, K., 1928. Die fossilen Dromiaceen und ihre Stammesgeschichte. *Palaeontologische Zeitschrift*, 10: 144–183.

Brönnimann, P., 1972. Remarks on the classification of fossil Anomuran coprolites. *Palaeontologische Zeitschrift*, 46: 99–103.

Buchs, D. M., Guex, J., Stucki, J. & Baumgartner, P. O., 2009. Paleocene Thalassinidea colonization in deep-sea environment and the coprolite *Palaxius osaensis* n. ichnosp. in Southern Costa Rica. *Revue de Micropaleontologie*, 52: 123–129.

Bujtor, L., 2012. A Valanginian crustacean microcoprolite ichnofauna from the shallow-marine hydrothermal vent site of Zengövárkony (Mecsek Mts., Hungary). *Facies*, 58: 249–260.

Bukowy, S., 1968. *Objaśnienia do szczegółowej mapy geologicznej Polski 1:50000, arkusz Wolbrom*. Wydawnictwa Geologiczne, Warszawa, 52 pp. [In Polish].

Bukowy, S. & Ślósarz, J., 1975. Palaeozoic and Mesozoic sequence at Smoleń near Pilica. *Biuletyn Instytutu Geologicznego*, 282: 419–448. [In Polish, English summary].

Buła, Z., 1994. Problemy stratygrafii i wykształcenia osadów starszego paleozoiku północno-wschodniego obrzeżenia Górnośląskiego Zagłębia Węglowego. *Prace Naukowe Uniwersytetu Śląskiego*, 1431: 31–57. [In Polish].

Buła, Z., 2002. *Geological Atlas of the Palaeozoic without the Permian in the Border Zone of the Upper Silesian and Małopolska Blocks. Explanatory Text*. Państwowy Instytut Geologiczny, Warszawa, 28 pp.

Buła, Z. & Habryn, R., 2011. Precambrian and Palaeozoic basement of the Carpathian Foredeep and the adjacent Outer Carpathians (SE Poland and western Ukraine). *Annales Societatis Geologorum Poloniae*, 81: 221–239.

Buła, Z., Jachowicz, M. & Żaba, J., 1997. Principal characteristics of the Upper Silesian Block and Małopolska Block border zone. *Geological Magazine*, 134: 669–677.

Collins, J. S. R. & Wierzbowski, A., 1985. Crabs from the Oxfordian sponge megafacies of Poland. *Acta Geologica Polonica*, 35: 73–88.

Dando, P. R., 2010. Biological communities at marine shallow-water vent and deep sites. In: Kiel, S. (ed.), *The Vent and Seep Biota – from Microbes to Ecosystems: Topics in Geobiology*, 33: 333–378.

Dando, P. R., Hughes, J. A., Leahy, Y., Taylor, L. J. & Zivanovic, S., 1995. Earthquakes increase hydrothermal venting and nutrient inputs into the Aegean. *Continental Shelf Research*, 15: 655–662.

Decho, A. W., 2000. Exopolymer microdomains as a structuring agent for heterogeneity within microbial biofilms. In: Riding, R. E. & Awramik, S. M. (eds), *Microbial Sediments*. Springer, Berlin, pp. 9–15.

Deines, P., Langmuir, D. & Hormon, R. S., 1974. Stable carbon isotope ratios and the existence of a gas phase in the evolution of carbonate ground waters. *Geochimica et Cosmochimica Acta*, 38: 1147–1164.

Dietl, G. & Schweigert, G., 2001. *Im Reich der Meerengel – Fossilien aus dem Nusplinger Plattenkalk*. Pfeil, München, 144 pp.

Draganescu, A., 1976. Constructional to corpuscular spongalgal, algal and coralgal facies in the Upper Jurassic carbonate formation of Central Dobrogea (the Casimcea Formation). In: Patrulius, D., Draganescu, A., Baltres, A., Popescu, B. & Radan, S. (eds), *International Colloquium Carbonate Rocks and Evaporites*, *Guidebook, Series 15.* Institute Geology and Geophysics of Romania, Bucharest, pp. 15–43.

Dromart, G., Gaillard, C. & Jansa, L. F., 1994. Deep-marine microbial structures in the Upper Jurassic of western Tethys. In: Bertrand-Sarfati, J. & Monty, C. (eds), *Phanerozoic Stromatolites II*. Kluwer, Dordrecht, pp. 345–391.

Dupraz, C. & Strasser, A., 1999. Microbialites and micro-encrusters in shallow coral bioherms (Middle to Late Oxfordian, Swiss Jura Mountains). *Facies*, 40: 101–130.

Dupraz, C., Reid, R. P., Braissant, O., Decho, A. W., Norman, R. S. & Visscher, P. T., 2009. Processes of carbonate precipitation in modern microbial mats. *Earth-Science Reviews*, 96: 141–162.

Dżułyński, S. & Sass-Gustkiewicz, M., 1982. The role of hydrothermal karst processes in the emplacement of sulfide ores. *Kras i Speleologia*, 4: 21–31.

Dżułyński, S. & Sass-Gustkiewicz, M., 1985. Hydrothermal karst phenomena as a factor in the formation of Mississippi Valley-type deposits. In: Wolf, K. H. (ed.), *Handbook of Strata-Bound and Stratiform Ore Deposits*, 13. Elsevier, Amsterdam, pp. 391–439.

Förster, R. & Matyja, B. A., 1986. Glypheoid lobsters, *Glyphaea (Glyphaea) muensteri* (Voltz), from the Oxfordian deposits of the Central Polish Uplands. *Acta Geologica Polonica*, 36: 317–324.

Gaillard, C., 1983. Les biohermes ŕ spongiaires et leur environment dans l'Oxfordien du Jura méridional. *Documents des Laboratoires de Géologie, Lyon*, 90: 1–515.

Gaillard, C., Bourseau, J. P., Boudeulle, M., Pailleret, P., Rio, M. & Roux, M., 1985. Les pseudo-biohermes de Beauvoisin (Drôme): un site hydrothermal sur la marge tèthysienne à l'Oxfordien? *Bulletin de la Société Géologique de France*, 8: 9–78.

Gaillard, C., Rio, M., Rolin, Y. & Roux, M., 1992. Fossil chemosynthetic communities related to vents or seeps in sedimentary basins: the pseudobioherms of southeastern France compared to other world examples. *Palaios*, 7: 451–465.

Gaździcki, A., Michalik, J. & Tomašových, A., 2000. *Parafavreina* coprolites from the uppermost Triassic of the Western Carpathians. *Geologica Carpathica*, 51: 245–250.

Gradziński, M., Motyka, J. & Górny, A., 2009. Artesian origin of a cave developed in an isolated horst: A case study of Smocza Jama (Kraków Upland, Poland). *Annales Societatis Geologorum Poloniae*, 79, 159–168.

Helm, C., 2005. Riffe und fazielle Entwicklung der *florigemma*-Bank (Korallenoolith, Oxfordium) im Süntel und östlichen Wesergebirge (NW-Deustchland). *Geologische Beiträge Hannover*, 7: 1–339.

Helm, C. & Schülke, I., 2004. Crustaceen-Koprolithen aus dem Korallenoolith (Oxfordium, Niedersächsisches Becken, NW-Deutschland). *Neues Jahrbuch für Geologie und Paläontologie – Monatshefte*, 8: 496–512.

Herrmann, R., 1996. Entwicklung einer oberjurassischen Karbonatplattform: Biofazies, Riffe und Sedimentologie im Oxfordium der Zentralen Dobrogea (Ost-Rumänien). *Berliner Geowissenschaftliche Abhandlungen*, E19: 1–102.

Jach, R. & Dudek, T., 2005. Origin of a Toarcian manganese carbonate/silicate deposit from the Krížna unit, Tatra Mountains, Poland. *Chemical Geology*, 224: 136–152.

Jacher-Śliwczyńska, K. & Schneider, J. C., 2004. Źródła mineralizacji galenowej obszaru śląsko-krakowskiego na podstawie analizy izotopowej Pb (U) – wyniki wstępne. In: Michalik, M., Jacher-Śliwczyńska, K., Skiba, M. & Michalik, J. (eds), *Datowanie minerałów i skał*, *VIII Ogólnopolska Sesja Naukowa*. WGGiOŚ AGH, ING UJ, Komitet Badań Czwartorzędu PAN, Kraków, pp. 50–55 [In Polish].

Jáger, V., Molnár F., Buchs, D. & Koděra, P., 2012. The connection between iron ore formations and "mud-shrimps" colonization around sunken wood debris and hydrothermal sediments in a Lower Cretaceous continental rift basin, Mecsek Mts., Hungary. *Earth-Science Reviews*, 114: 250–278.

Jeng, M. S., Ng, N. K. & Ng, P. K. L., 2004. Feeding behaviour: Hydrothermal vent crabs feast on sea 'snow'. *Nature*, 423: 969.

Kato, H., Takahashi, T. & Taira, M., 2011. Additions to macruran decapod crustaceans from the Upper Jurassic of Somanakamura Group, northeast Japan. *Neues Jahrbuch für Geologie und Paläontologie – Abhandlungen*, 260: 185–190.

Keupp, H., Jenisch, A., Herrmann, R., Neuweiler, F. & Reitner, J., 1993. Microbial crusts a key to the environmental analysis of fossil spongiolites? *Facies*, 29: 41–54.

Kietzmann, D. A., Blau, J., Fernández, D. E. & Palma, R. M., 2010. Crustacean microcoprolites from the Upper Jurassic–Lower Cretaceous of the Neuquén basin, Argentina: systematic and biostratigraphic implications. *Acta Palaeontologica Polonica*, 55: 277–284.

Kochman, A., 2010. *Wpływ kompakcji na architekturę facjalną późnojurajskiego basenu południowej części Wyżyny Krakowsko-Częstochowskiej*. Unpublished PhD. Thesis, Faculty of Geology, Geophysics and Environment Protection, AGH University of Science and Technology, 117 pp. [In Polish].

Krautter, M., 1998. Ecology of siliceous sponges: application to

the environmental interpretation of the Upper Jurassic sponge facies (Oxfordian) from Spain. *Cuadernos de Geología Ibérico*, 24: 223–239.

Krobicki, M. & Zatoń, M., 2008. Middle and Late Jurassic roots of brachyuran crabs: Palaeoenvironmental distribution during their early evolution. *Palaeogeography, Palaeoclimatology, Palaeoecology*, 263: 30–43.

Kutek, J. & Zapaśnik, T., 1992. Bydlin, large scale synsedimentary mass movements of Late Oxfordian. In: Matyja, B. A., Wierzbowski, A. & Radwański, A. (eds), *Oxfordian and Kimmeridgian joint working groups meeting*. *International Subcommision Jurassic Stratigraphy, Guidebook and Abstracts*. Institute of Geology, University of Warsaw, Warszawa, pp. 22–26.

Kutek, J., Wierzbowski, A., Bednarek, J., Matyja, B. A. & Zapaśnik, A., 1977. Notes on the Upper Jurassic stratigraphy in the Polish Jura chain. *Przegląd Geologiczny*, 25: 438–445. [In Polish, English summary].

Lehman, R., 2007. Crustacean coproliths from topmost Jurassic or basal Cretaceous deposits of the northwestern Pacific. *Initial Reports of the Deep Sea Drilling Project*, 32: 827–833.

Matyszkiewicz, J., 1996. The significance of Saccocoma-calciturbidites for the analysis of the Polish Epicontinental Late Jurassic Basin: an example from the Southern Cracow-Wieluń Upland (Poland). *Facies*, 34: 23–40.

Matyszkiewicz, J., 1997. Microfacies, sedimentation and some aspects of diagenesis of Upper Jurassic sediments from the elevated part of the Northern peri-Tethyan Shelf: a comprative study on the Lochen area (Schwäbische Alb) and the Cracow area (Cracow-Wieluń Upland, Poland). *Berliner Geowissenschaftliche Abhandlungen*, E 21: 1–111.

Matyszkiewicz, J. & Krajewski, M., 1996. Lithology and sedimentation of Upper Jurassic massive limestones near Bolechowice, Kraków-Wieluń Upland, south Poland. *Annales Societatis Geologorum Poloniae*, 66: 285–301.

Matyszkiewicz, J., Kochman, A. & Duś, A., 2012. Influence of local sedimentary conditions on development of microbialites in the Oxfordian carbonate buildups from the southern part of the Kraków-Częstochowa Upland (south Poland). *Sedimentary Geology*, 263–264: 109–132.

Matyszkiewicz, J., Krajewski, M. & Kędzierski, J., 2006a. Origin and evolution of an Upper Jurassic complex of carbonate buildups from Zegarowe Rocks (Kraków-Wieluń Upland, Poland). *Facies*, 52: 249–263.

Matyszkiewicz, J., Krajewski, M., Tyc, A., Król, K., Kędzierski, J., Jędrys, J. & Świąder, J., 2004. Facial development of the Upper Jurassic complex of the Zegarowe Rocks near Smoleń (Kraków-Wieluń Upland; southern Poland). In: Partyka, J. (ed.), *Zróżnicowanie i przemiany środowiska przyrodniczo-kulturowego Wyżyny Krakowsko-Częstochowskiej*. Ojcowski Park Narodowy, Ojców, pp. 35–42. [In Polish, English summary].

Matyszkiewicz, J., Krajewski, M. & Żaba, J., 2006b. Structural control on the distribution of Upper Jurassic carbonate buildups in the Kraków-Wieluń Upland (South Poland). *Neues Jahrbuch für Geologie und Paläontologie Monatshefte*, 3: 182–192.

Merta, T., 1972. Facial development of the Opoczno limestones (Oxfordian, NW Mesozoic margin of the Holy Cross Mts). *Acta Geologica Polonica*, 22: 29–44. [In Polish, English summary].

Meyer, R. K. F., 1975. Mikrofazielle Untersuchungen in Schwamm-Biohermen und -Biostromen des Malm Epsilon (Ober-Kimmeridge) und obersten Malm Delta der Frankenalb. *Geologische Blätter für Nordost-Bayern*, 25: 149–177.

Moczydłowska, M., 1997. Proterozoic and Cambrian successions in Upper Silesia: an Avalonian terrane in southern Poland. *Geological Magazine*, 134: 679–689.

Monty, C., 1967. Distribution and structure of recent stromatolitic algal mats, eastern Andros Island, Bahamas. *Annales de la Société Géologique de Belgique*, 90: 55–100.

Morad, S., 1998. Carbonate cementation in sandstones: distribution patterns and geochemical evolution. In: Morad, S. (ed.), *Carbonate Cementation in Sandstones*. *International Association of Sedimentologists*, *Special Publication*, 26: 1–26.

Müller, P., Krobicki, M. & Wehner, G., 2000. Jurassic and Cretaceous primitive crabs of the family Prosopidae (Decapoda: Brachyura) – their taxonomy, ecology and biogeography. *Annales Societatis Geologorum Poloniae*, 70: 49–79.

Neuweiler, F., Gautret, P., Thiel, V., Langes, R., Michaelis, W. & Reitner, J., 1999. Petrology of Lower Cretaceous carbonate mud mounds (Albian, N. Spain): insights into organomineralic deposits of the geological record. *Sedimentology*, 46: 837–859.

Neuweiler, F., Rutsch, M., Geipel, G., Reimer, A. & Heise, K. H., 2000. Soluble humic substances from in situ precipitated micro-crystalline carbonate, internal sediment, and spar cement in a Cretaceous carbonate mud-mound. *Geology*, 28: 851–854.

Nitzopoulos, G., 1973. *Faunistisch-ökologische, stratigraphische und sedimentologische Untersuchungen am Schwammstotzenkomplex bei Spielberg am Hahnenkamm (Ob. Oxfordien, Südliche Frankenalb)*. Unpublished PhD. Thesis, Technische Universität Berlin, 155 pp.

Olivier, N., Colombié, C., Pittet, B. & Lathuilière, B., 2010. Microbial carbonates and corals on the marginal French Jura platform (Late Oxfordian, Molinges section). *Facies*, 57: 469–492.

Olivier, N., Hantzpergue, P., Gaillard, C., Pittet, B., Leinfelder, R. R., Schmid, D. U. & Werner, W., 2003. Microbialite morphology, structure and growth: a model of the Upper Jurassic reefs of the Chay Peninsula (western France). *Palaeogeography, Palaeoclimatology, Palaeoecology*, 193: 383–404.

O'Neil, J. R., Clayton, R. N. & Mayeda, T. K., 1969. Oxygen isotope fractionation in divalent metal carbonates. *Journal of Chemical Physics*, 51: 5547–5558.

Prezbindowski, D. R. & Tapp, J. B., 1989. Asymmetric dissolution textures as evidence of subaerial exposure. *Journal of Sedimentary Petrology*, 59: 835–838.

Powell, R. R., 1974. The functional morphology of the fore-guts of the thalassinid crustaceans, *Callianassa californiensis* and *Upogebia pugettensis*. *University of California Publications in Zoology*, 102: 1–47.

Pulina, M., Żaba, J. & Polonius A., 2005. Relation between karst forms of Smoleń-Niegowonice Range and tectonic activity of Cracow-Wieluń Upland base. *Kras i Speleologia*, 11: 39–83. [In Polish, English summary].

Reitner, J., 1994. Mikrobialith-Porifera Fazies eines Exogyren/Korallen Patchreefs des Oberen Korallenooliths im Steinbruch Langenberg bei Oker (Niedersachsen). *Berliner Geowissenschaftliche Abhandlungen*, E13: 397–417.

Reitner, J. & Schumann-Kindel, G., 1997. Pyrite in mineralized sponge tissue-Product of sulfatereducing sponge related bacteria? *Facies*, 36: 272–276.

Reolid, M., 2011. Interactions between microbes and siliceous sponges from Upper Jurassic buildups of External Prebetic (SE Spain). In: Reitner, J., Quéric, N. V. & Arp, G. (eds), *Advances in Geobiology of Stromatolite Formation*. *Lecture Notes in Earth Sciences*, 131: 319–330.

Reolid, M., Gaillard, C., Olóriz, F. & Rodríguez-Tovar, F. J.,

2005. Microbial encrustations from the Middle Oxfordian–earliest Kimmeridgian lithofacies in the Prebetic Zone (Betic Cordillera, southern Spain): characterization, distribution and controlling factors. *Facies*, 50: 529–543.

Riding, R., 1999. The term stromatolite: towards an essential definition. *Lethaia*, 32: 321–330.

Riding, R., 2000. Microbial carbonates: the geological record of calcified bacterial-algal mats and biofilms. *Sedimentology*, 47: 179–214.

Riding, R., 2002. Structure and composition of organic reefs and carbonate mud mounds: concepts and categories. *Earth-Science Reviews*, 58: 163–231.

Schmid, D. U., 1996. Marine Mikrobolithe und Mikroinkrustierer aus dem Oberjura. *Profil*, 9: 101–251.

Schweigert, G., 2010. New genera and species of "thalassinideans" (Crustacea: Decapoda: Axiidea, Gebiidea) from the Upper Jurassic of Eichstätt and Brunn (S Germany). *Archaeopteryx*, 7: 21–30.

Schweigert, G. & Koppka, J., 2011. Decapods (Crustacea: Brachyura) from the Jurassic of Germany and Lithuania, with descriptions of new species of *Planoprosopon* and *Tanidromites*. *Neues Jahrbuch für Geologie und Paläontologie – Abhandlungen*, 260: 221–235.

Schweigert, G., Seegis, D. B., Fels, A. & Leinfelder, R. R., 1997. New internally structured decapod microcoprolites from Germany (Late Triassic/Early Miocene), Southern Spain (Early/Middle Jurassic) and Portugal (Late Jurassic): Taxonomy, palaeocology and evolutionary implications. *Palaeontologische Zeitschrift*, 71: 51–69.

Senowbari-Daryan, B., Gaillard, C. & Peckmann, J., 2007. Crustacean microcoprolites from Jurassic (Oxfordian) hydrocarbon-seep deposits of Beauvoisin, southeastern France. *Facies*, 53: 229–238.

Sibson, R. H., 1987. Earthquake rupturing as a hydrothermal mineralizing agent. *Geology*, 15: 701–704.

Sudarikov, S. M. & Galkin, S. V. 1995. Geochemistry of the Snake Pit vent field and its implications for vent and non-vent fauna. In: Parson, L. M., Walker, C. L. & Dixon, D. R. (eds), *Hydrothermal Vents and Processes. Geological Society Special Publication*, 87: 319–327.

Szulc, J., Gradziński, M., Lewandowska, A. & Heunisch, C., 2006, The Upper Triassic crenogenic limestones in Upper Silesia (southern Poland) and their paleoenvironmental context. In: Alonso-Zarza, A. M. & Tanner, L. H. (eds), *Paleoenvironmental Record and Applications of Calcretes and Palustrine Carbonates. Geological Society of America Special Paper*, 416: 133–151.

Van Dover, C. L., 1995. Ecology of Mid-Atlantic Ridge hydrothermal vents. In: Parson, L. M., Walker, C. L. & Dixon, D. R. (eds), *Hydrothermal Vents and Processes. Geological Society Special Publication*: 87: 257–294.

Vierek, A., 1997. Origin of Upper Jurassic sediments from Bydlin quarry (southern Poland). *Przegląd Geologiczny*, 45: 428–430. [In Polish, English summary].

Vierek, A., Heliasz, Z. & Zieliński, T., 1994 Górnojurajskie osady podmorskich spływów; stanowisko 4 – Bydlin. In: Malik, K., Bardziński, W., Teper, E., Waga, J. M. & Zieliński, T. (eds), *Sedymentacja normalna, katastroficzna i wyjątkowa; procesy i produkty*. III Krajowe Spotkania Sedymentologów, Wydział Nauk o Ziemi Uniwersytetu Śląskiego, Sosnowiec, pp. 26–30. [In Polish].

Wright, V. P., 1991. Palaeokarst types, recognition, controls and associations. In: Wright, V. P., Esteban, M. & Smart, P. L. (eds), *Palaeokarsts and Palaeokarstic Reservoirs*. *Postgraduate Research Institut for Sedimentology, Occasional Publication Series No. 2.* University of Reading, Reading, pp. 56–88.

Żaba, J., 1994. Mesoscopic flowers structures in the Lower Palaeozoic deposits of the NE border of the Upper Silesia Coal Basin – a result of the transpresional shearing in the Kraków-Myszków (Hamburg-Kraków) dislocation zone (SW Poland). *Przegląd Geologiczny*, 42: 643–648. [In Polish, English summary].

Żaba, J., 1995. Strike-slip faults at the edge zone of Upper Silesia and Małopolska blocks (southern Poland). *Przegląd Geologiczny*, 43: 838–842. [In Polish, English summary].

Żaba, J., 1996. Late Carboniferous strike-slip activity at the boundary zone of Upper Silesia and Małopolska blocks (southern Poland). *Przegląd Geologiczny*, 44: 173–180. [In Polish, English summary].

Żaba, J., 1999. The structural evolution of Lower Palaeozoic succession in the Upper Silesia Block and Małopolska Block border zone, southern Poland. *Prace Państwowego Instytutu Geologicznego*, 166: 1–162. [In Polish, English summary].